T_0 and T_{min} in the pure metals, which seems to be lost in the alloy K-Na. However, in contrast to the situation in the noble metals where T_{min} for the alloys was always approximately equal to T_{min} in the host, we see that T_{min} in K-Na is quite different (greater by a factor of 2) from T_{min} in pure K. This coupled with the fact that in the K-Rb alloy, where we feel that the impurity scattering is quite isotropic, the temperature variation of n^* is almost a continuation below T_{min} of the situation in pure K weighs favorably towards the residual impurity scattering being the explanation of the minimum in n^* in these metals.

V. CONCLUSION

The measurements of the Hall coefficients of the three alkali metals, Li, Na, and K, yield values of n^* at room temperature, very close to unity, as expected from the free-electron model. At lower temperatures, n^* falls slightly below unity and it was proposed that in K and Na the reason for this behavior is the anisotropic phonon spectrum. In Li in its bcc phase, n^* varies more severely, which is consistent with this metal having the most distorted Fermi surface. The variation of n^* in the two alloys was shown to be consistent with the p state being highest at the zone boundary in potassium. In the three pure metals (Li in its hexagonal phase) a minimum in n^* was observed at low temperatures. Two possible explanations were offered for this effect, and although we felt that it was impossible to decide absolutely on the origin, the arguments we presented seem to favor residual impurity scattering as the explanation.

PHYSICAL REVIEW VOLUME 185, NUMBER 3 15 SEPTEMBER 1969

Photoemission Studies of the Noble Metals. I. Copper*

W. F. KROLIKOWSKI†
Stanford University, Stanford, California 94305
and
Cogar Corporation, Poughkeepsie, New York 12600

AND

W. E. SPICER
Stanford University, Stanford, California 94305

(Received 29 January 1969)

New photoelectric energy-distribution and quantum-yield measurements have been made on carefully prepared clean Cu films in the range of photon energies 4.8–11.6 eV. The energy-distribution curves (EDC's) are found to be rich in structure. They give no evidence that conservation of $\mathbf{k}$ provides an important optical selection rule; rather, it appears that the model of nondirect transition suffices to explain the data. [In this model only conservation of energy and the product of the initial and final optical densities of states (ODS) are important in determining the optical transition probability.] By combining our new results with those obtained earlier by Berglund and Spicer from cesiated Cu, an ODS has been constructed for copper over a range of ~20 eV. Four peaks or shoulders are found in the ODS for the d states, which correlate well in position with structure in the density of states calculated by Mueller and by Snow. These peaks or shoulders are located approximately 2.3, 2.9, 3.7, and 4.5 eV below the Fermi surface. Comparison is also made between the ODS and information on the density of states obtained by x-ray and ion-neutralization studies. Using the ODS, a large number of EDC's are calculated and found to agree well with experiment. In addition, reasonable agreement is found with experiment when the ODS is used to calculate the quantum yield, the electron-electron scattering length, and the imaginary part of the dielectric constant.

I. INTRODUCTION

NEW photoemission measurements on clean Cu have been made in the range of photon energies 4.8–11.6 eV. By combining these new results with the earlier results of Berglund and Spicer[1,2] on cesiated Cu, we have constructed an optical density of states (ODS) for Cu that is consistent with the calculated band structure, the optical constant ϵ_{2b}, the electron-electron scattering length, the quantum yield, and the photoelectric energy-distribution curves (EDC's).

* Work supported by The National Aeronautics and Space Administration, the National Science Foundation, and the Advanced Research Projects Agency through the Center for Materials Research at Stanford University.

† Based largely on a thesis submitted by W. F. Krolikowski to Stanford University in partial fulfillment of the requirements for the Ph.D. degree.

[1] C. N. Berglund and W. E. Spicer, Phys. Rev. 136, A1030 (1964).

[2] C. N. Berglund and W. E. Spicer, Phys. Rev. 136, A1044 (1964).

This work differs from the previous photoemission study of Cu by Berglund and Spicer[1,2] in two important features. The previous experimental work was done on cesium-treated Cu; the present work is done on clean Cu without cesium. In the prior work on Cu, a method of analysis was developed in terms of "nondirect" transitions[1–5]; however, because all calculations were done by hand, it was not possible to calculate the EDC's for all values of photon energy. In the present work, using the nondirect model, machine calculations were used to produce EDC's for all values of $h\nu$ for clean as well as cesiated Cu. In addition, EDC's were calculated to compare with the recent results of Vehse and Arakawa[6] at values of photon energy higher than those used in Berglund and Spicer[2] or in the present experimental work. As in the earlier study, calculations have also been made on the absolute value of quantum yield and relative values for the imaginary part of the dielectric constant ϵ_2 and the electron-electron scattering length. Thus, there are a large number of calculated results which can be compared with experiment. Such a detailed comparison with experiment is warranted in view of the most surprising and controversial feature of the earlier work on Cu and certain other materials.[3–8] This was the discovery that, for transitions from the d band, conservation of crystal momentum $\mathbf{k}$ does not provide an important optical selection rule. This is in contrast to the situation for transitions from the s- and p-derived bands in Cu where a transition was observed[2] in which conservation of $\mathbf{k}$ did provide an important optical selection rule, i.e., the optical transition was direct. The lack of importance of $\mathbf{k}$ conservation for the d transitions is also in contrast to the situation in such crystalline materials as Ge and GaAs, where detailed photoemission studies show that the strong optical transitions are direct.[9]

A principal object of the work reported is to test the "nondirect-transition constant-matrix-element" model developed by Spicer[10] and Berglund and Spicer[1,2] even further. In this model it is assumed that $\mathbf{k}$ conservation does not provide an important optical selection rule, and that the matrix elements are independent of the initial state from which an electron is excited (this will be outlined in more detail in Sec. III).

II. EXPERIMENTAL METHODS

Photoelectric yield and energy-distribution measurements have been made at photon energies up to 11.6 eV on Cu films evaporated and tested *in situ* at a pressure of about 2×10^{-9} Torr. The specimens were evaporated and tested in a continuously pumped oil-free metal and glass chamber, which was evacuated by a combination of sputter-ion, titanium-sublimation, and cryogenic-pumping techniques. The light source was a McPherson model 225 vacuum ultraviolet monochromator; light was admitted into the photoemission chamber through a cleaved Harshaw LiF window, which had a high-energy cutoff of $\sim$11.6 eV. The experimental photodiode used to measure the EDC's and the quantum yield was located inside the photoemission chamber. The uv light entered the photodiode after passing through the LiF window that was sealed to the walls of the photoemission chamber. The photodiode was of the simple (easy to manufacture), cylindrical type described earlier by Apker *et al.*[11] and Spicer.[12] Although the cylindrical geometry is quite different from the ideal geometry of a very small emitter in a very large spherical collector with a small light hole, little difference has been found to date in the EDC's obtained from either geometry. The resolution in the EDC's is 0.1—0.2 eV.

The possible effect of contamination has been essentially eliminated since, at the low pressures used during the experiments, several EDC's could be measured on a freshly prepared film before a monolayer of gas could form on the surface. The EDC's taken within minutes after evaporation had slightly sharper features than the EDC's taken on the same film hours or days later. However, the difference in structure between a fresh film and an old film was on the order of 1%, a negligible amount of deterioration. The Cu films were, typically, several thousand angstroms thick, and were evaporated inside the collector can onto a highly polished Cu, Ag, or Au substrate. The EDC's were found to be independent of the substrate material. High-purity Cu films were evaporated from well-outgassed beads which had been preformed on Mo filaments. Inferior EDC's (with less pronounced structure) were obtained if the entire copper bead was evaporated; thus, care was taken to stop the evaporation while some Cu still covered the Mo wire. Typically, several thousand angstroms of Cu were evaporated in about 30 sec; the maximum pressure during evaporation was always less than 5×10^{-9} Torr. The inside of the collector can was coated with copper during the emitter evaporation, thereby eliminating the possibility of regions of oxide on the surface of the collector giving work-function variations. After the evaporation the Cu bead was withdrawn from inside the collector can by mechanical motions inside the high-vacuum chamber.

The EDC's were measured directly using an ac modulation technique similar in principle to that described

[3] W. E. Spicer, Phys. Rev. **154**, 384 (1967).
[4] W. E. Spicer, in *A Survey of Phenomena in Ionized Gases, Invited Papers* (International Atomic Energy Agency, Vienna, 1968), pp. 271–290.
[5] W. E. Spicer, in *Optical Properties of Solids*, edited by F. Abelès (North-Holland Publishing Co., Amsterdam, to be published).
[6] R. C. Vehse and E. T. Arakawa, Oak Ridge National Laboratory Report No. ORNL–TM–2240, 1968 (unpublished).
[7] D. E. Eastman and W. F. Krolikowski, Phys. Rev. Letters **21**, 623 (1968).
[8] D. E. Eastman, J. Appl. Phys. **40**, 1387 (1969).
[9] W. E. Spicer and R. C. Eden, in *Proceedings of the Ninth International Conference on Semiconductors, Moscow* (Nauka, Leningrad, 1968), p. 65.
[10] W. E. Spicer, Phys. Rev. Letters **11**, 243 (1963).
[11] L. Apker, E. A. Taft, and J. Dickey, J. Opt. Soc. Am. **43**, 78 (1953).
[12] W. E. Spicer, J. Phys. Chem. Solids **22**, 365 (1961).

earlier by Spicer and Berglund.[13] The absolute quantum yield was obtained at a given photon energy by comparing the photocurrent from the Cu specimen to the photocurrent from a Cs_3Sb tube (calibrated by Koyama of the Stanford University laboratory) which could be moved in and out of the incident light beam. In obtaining the quantum yield per absorbed photon, account was taken of the transmission of the LiF window of the experimental chamber as well as of the Cu reflectivity.[14] The transmission of the LiF window could be measured before and after each experiment. A more detailed description of the experimental apparatus and the measurement techniques has been presented elsewhere.[15]

III. MODEL FOR PHOTOEMISSION AND IMAGINARY PART OF DIELECTRIC CONSTANT

In this section we derive a mathematical model describing the photoemission process for a material with a free-electron-like conduction band and a semiclassical threshold function. The model is based upon the nondirect transitions.[1–5] The method of analysis will proceed as follows: We calculate (a) the probability of exciting an electron at a depth x from the surface,[5] (b) the probability that the electron will then be excited to an energy E in the conduction band, and (c) the probability that the electron excited to energy E will then travel to the surface without suffering an inelastic electron-electron scattering event, and escape into vacuum. The result of this analysis will yield the photoelectric energy distributions and the photoelectric yield for nonscattered electrons in terms of the density of states, the electron-electron scattering length, and other physical parameters.

Let us begin by assuming that a monochromatic beam of photon energy $h\nu$ is normally incident upon a semi-infinite solid or liquid surface in the x direction of a rectangular coordinate system. Some of the light will be reflected, and some will be absorbed within the material. We assume that the total energy of a single photon is given to a single electron. If x is the distance from the surface, the spatial distribution of excited electrons is given by

$$G(x,h\nu)=I^i(h\nu)[1-R(h\nu)]\alpha(h\nu)e^{-\alpha(h\nu)x}, \quad (1)$$

where $R(h\nu)$ is the reflection coefficient at normal incidence and I^i is the incident photon flux. $G(x,h\nu)$ is a generation rate, giving the number of electrons generated in the incident between x and $x+dx$ per unit area per unit time. The electrons represented by $G(x,h\nu)$ are excited from filled states in the valence band to empty states in the conduction band. According to the model of nondirect transitions with constant matrix elements, the probability P of excitation of an electron to energy E from energy $E-h\nu$ is given by

$$P(E,h\nu)dE=MN_C(E)N_V(E-h\nu)dE, \quad (2)$$

where M is a constant, N_V is the valence-band ODS, and N_C is the conduction-band ODS. Equation (2) represents an important fundamental assumption in the analysis, in that it states that the transition probability is dependent only upon the optical density of valence states at energy $E-h\nu$ and the optical density of conduction states at energy E, and is not dependent upon the wave vector $\mathbf{k}$. A possible difference between the ODS and the actual density of states is perhaps now apparent. If there is a constant matrix element enhancing the transition from initial states at energy E to all final states in the energy range of the measurement, the valence ODS at E will appear to be greater than the actual density of states. A similar enhancement (or reduction) is possible for the final ODS. For the purpose of this analysis, it will be sufficient to assume that all states below the Fermi level are filled, and that all states above the Fermi level are empty. Normalizing $P(E,h\nu)$ to unity, we find

$$P(E,h\nu)=N_C(E)N_V(E-h\nu)\Big/\int_{E_F}^{E_F+h\nu}N_C(E)N_V(E-h\nu)dE, \quad (3)$$

where E_F is the Fermi level. Combining Eqs. (2) and (3), the generation rate of electrons excited to energy E at depth x is

$$G(E,x,h\nu)=I^i(h\nu)[1-R(h\nu)]\alpha(h\nu)e^{-\alpha(h\nu)x}N_C(E)N_V(E-h\nu)\Big/\int_{E_F}^{E_F+h\nu}N_C(E)N_V(E-h\nu). \quad (4)$$

In the discussion to follow, we shall assume that the conduction band Cu can be approximated by a single spherical conduction band and that the velocity of an excited electron is that associated with this spherical conduction band. This approximation is consistent with the energy-band diagram shown in Fig. 1, which indicates that the conduction bands of Cu are largely free-electron-like well above the Fermi level. Structure has been found in the ODS ~2.0 eV above the Fermi surface; however, as a first approximation we shall use the spherical band to determine the group velocity of the electrons in this energy range. The hot electrons originating at the point $r_0(x_0,y_0,z_0)$ [see Fig. 2(a)] will travel

[13] W. E. Spicer and C. N. Berglund, Rev. Sci. Instr. **35**, 1665 (1964).

[14] H. Enrenreich and H. R. Philipp, Phys. Rev. **128**, 1622 (1962).

[15] W. Krolikowski, Ph.D. thesis, Stanford University, 1967 (unpublished); Stanford Electronics Laboratories Report No. T.R. 5281-1, SEL-67-039 (unpublished). Copies may be obtained by writing University Microfilms Library Services, Xerox Corp., Ann Arbor, Mich. 48106, and asking for Document No. 65-11813. Xerox copy costs $16.65 and microfilm costs $4.75 (plus handling and postage).

in all directions with equal probability, and will have a group velocity $\mathbf{v}_g(E)$ appropriate to a free-electron band:

$$|\mathbf{v}_g(E)| = (2/m)^{1/2}(E-E_B)^{1/2}, \quad (5)$$

where m denotes the electron mass and E_B denotes the energy of the bottom of the free-electron-like conduction band.

Let us now calculate the number of electrons that will travel to the surface without suffering an inelastic electron-electron collision, overcome the potential barrier $W=E_V-E_B$, and escape into the vacuum. In this step, we use the well-known semiclassical escape-cone analysis[1,16,17] [see Figs. 2(b) and 3], by which an electron can escape if it arrives at the surface with a normal velocity that satisfies the condition

$$(1/2m)(v_g)_x^2 \geq W = E_V - E_B, \quad (6)$$

where E_V is the energy at the vacuum level. The fraction of electrons excited to energy E that satisfies this condition is given by the velocity cone of Fig. 3, which shows that all electrons in the solid angle

$$\theta_0 = \cos^{-1}(W/E)^{1/2}, \quad E \geq W \quad (7)$$

are candidates for escape into vacuum. However, some of these electrons will suffer inelastic electron-electron collisions on the way to the surface. For much of the present analysis, we shall consider only those electrons that reach the surface without encountering such a scattering event. In addition, we shall neglect electron-phonon-scattering, which we find to be negligible in Cu compared to electron-electron scattering for hot electrons more than a few eV above the Fermi level.

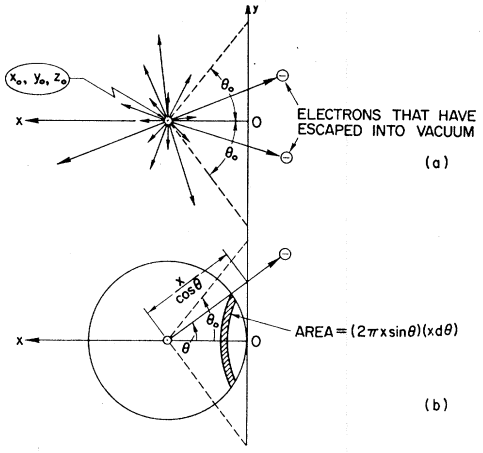

FIG. 1. (a) Photoemission escape process. The direction of an arrow represents the direction of the velocity, and the tip of the arrow indicates where the electron scatters with another electron. The dashed line shows the velocity cone. Electrons in the velocity cone can escape from the solid if they do not scatter before reaching the surface. (b) Geometry used in calculating the escape probability.

[16] R. H. Fowler, Phys. Rev. 38, 45 (1931).
[17] L. A. DuBridge, Phys. Rev. 39, 108 (1932).

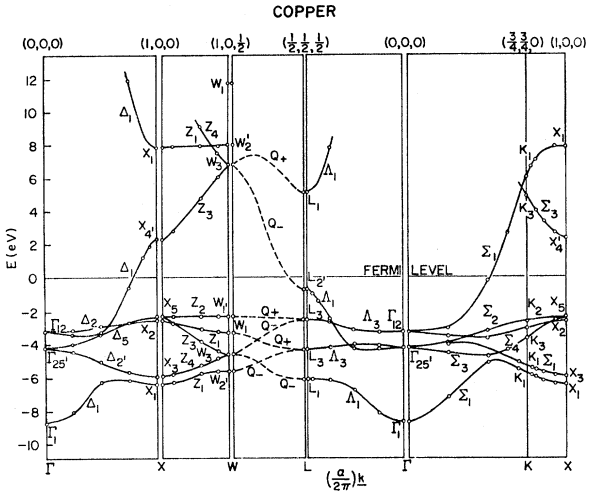

FIG. 2. Calculated band structure of Cu [after Segal (Ref. 49)].

An electron starting at point $\mathbf{r}_0(x_0,y_0,z_0)$ and traveling at an angle θ with respect to the x axis must travel a distance $|\mathbf{r}-\mathbf{r}_0|$ before reaching the surface, where

$$|\mathbf{r}-\mathbf{r}_0| = x/\cos\theta, \quad (8)$$

as seen from Fig. 1(b). The probability Q that an electron does not scatter before reaching the surface is given by

$$Q = e^{-|\mathbf{r}-\mathbf{r}_0|/L(E)} = e^{-x/L(E)\cos\theta}, \quad (9)$$

where $L(E)$ is the electron-electron scattering length. The fraction of electrons in the solid angle between θ and $\theta+d\theta$ is determined from Fig. 1 to be $\frac{1}{2}\sin\theta\, d\theta$. Thus, the fraction of electrons from (x,y_0,z_0) that can escape is

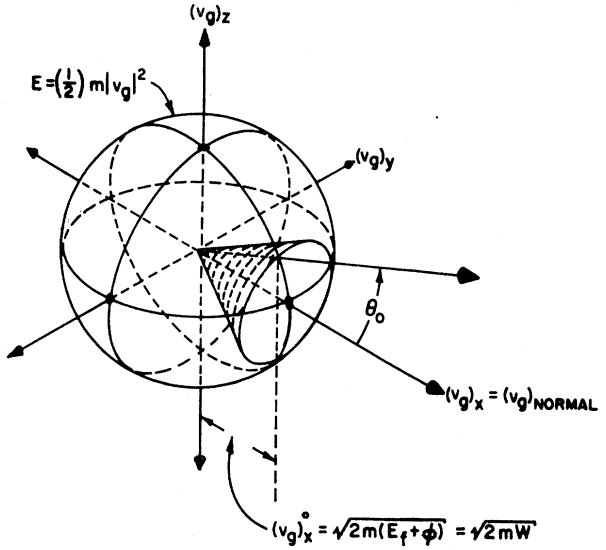

FIG. 3. Velocity cone used in the calculation of the semiclassical escape function. The surface of the material is in the positive x direction.

given by $F(E,x)$,where

$$F(E,x)=\begin{bmatrix}\text{fraction of electrons}\\ \text{at } E \text{ and } x \text{ that}\\ \text{escape without scattering}\end{bmatrix}$$

$$=\int_{\theta=0}^{\theta_0}\tfrac{1}{2}\sin\theta\, e^{-x/L(E)\cos\theta}d\theta. \quad (10)$$

Since the generation rate at depth x and energy E is $G(E,x,h\nu)$, the total number of nonscattered electrons that escape is given by $\mathfrak{N}'(E,x,h\nu)$, where

$$\mathfrak{N}'(E,x,h\nu)=G(E,x,h\nu)F(E,x). \quad (11)$$

Summing contributions from all possible values of x, we obtain

$$\mathfrak{N}'(E,h\nu)=\int_{x=0}^{\infty}\mathfrak{N}'(E,x,h\nu)dx$$

$$=\int_{x=0}^{\infty}G(E,x,h\nu)F(E,x)\,dx, \quad (12)$$

where $\mathfrak{N}'(E,h\nu)$ is the number of electrons photoemitted at energy E due to the incident photon flux $I^i(h\nu)$. Normalizing to the absorbed photon flux $I_0=I^i(h\nu)\times[1-R(h\nu)]$,

$$\mathfrak{N}(E,h\nu)=\frac{\mathfrak{N}'(E,h\nu)}{I_0(h\nu)}=\frac{\mathfrak{N}'(E,h\nu)}{I^i(h\nu)[1-R(h\nu)]}, \quad (13)$$

where $\mathfrak{N}(E,h\nu)$, the EDC, is the number of electrons photoemitted at energy E per absorbed photon per eV. Combining Eqs. (4), (10), (12), and (13), we find that $\mathfrak{N}(E,h\nu)$ is given by

$$\mathfrak{N}(E,h\nu)=\tfrac{1}{2}\alpha(h\nu)\left(N_C(E)N_V(E-h\nu)\Big/\int_{E}^{E_F+E}N_C(E)N_V(E-h\nu)dE\right)$$
$$\times\int_{x=0}^{\infty}dx\int_{\theta=0}^{\theta_0}\sin\theta\, e^{-[\alpha(h\nu)+1/L(E)\cos\theta]x}\,d\theta. \quad (14)$$

By making the substitution $\beta=\cos\theta$, and changing the order of integration, we find that Eq. (14) becomes

$$\mathfrak{N}(E,h\nu)=\tfrac{1}{2}\alpha(h\nu)\left(N_C(E)N_V(E-h\nu)\Big/\int_{E_F}^{E_F+h\nu}N_C(E)N_V(E-h\nu)dE\right)$$
$$\times\int_{\cos\theta_0}^{1}\left(\int_{x=0}^{\infty}e^{-[\alpha(h\nu)+1/L(E)\beta]x}\,dx\right)d\beta. \quad (15)$$

The integrals are easily evaluated; we obtain

$$\mathfrak{N}(E,h\nu)$$
$$=\frac{1}{2}\left((1-\cos\theta)-\frac{1}{\alpha(h\nu)L(E)}\ln\frac{\alpha(h\nu)L(E)+1}{\alpha(h\nu)L(E)\cos\theta+1}\right)$$
$$\times N_C(E)N_V(E-h\nu)\Big/\int_{E_F}^{E_F+h\nu}N_C(E)N_V(E-h\nu)dE. \quad (16)$$

Equation (16) is actually the final objective of this derivation, but the expression can be factored into the more understandable form

$$\mathfrak{N}(E,h\nu)=C[\alpha(h\nu)L(E),T_F(E)]T_F(E)$$
$$\times\frac{\alpha(h\nu)L(E)}{\alpha(h\nu)L(E)+1}N_C(E)N_V(E-h\nu)\Big/$$
$$\int_{E_F}^{E+h\nu}N_C(E)N_V(E-h\nu)dE, \quad (17)$$

where

$$T_F(E)=\tfrac{1}{2}(1-\cos\theta_0) \quad (18)$$

is the semiclassical threshold function and

$$C[\alpha(h\nu)L(E),T_F(E)]$$
$$=\frac{\alpha L+1}{\alpha L}-\frac{\alpha L+1}{2(T_F)(\alpha L)^2}\ln\frac{\alpha L+1}{\alpha L+1-2\alpha LT_F}. \quad (19)$$

The factor $T_F(E)\times\alpha(h\nu)L(E)/[\alpha(h\nu)L(E)+1]$ in Eq. (17) is just what would be obtained if all the electrons in the velocity core had velocities directed normal to the surface. The correction factor C of Eq. (19) gives the adjustment that must be made when the angular distribution of electrons is taken into account. For any values of αL and T_F, the correction factor C can vary[18] only between 0.5 and 1.0.

The quantum yield $Y(h\nu)$ is the area under the EDC, and is given by

$$Y(h\nu)=\int_{E_V}^{h\nu}N(E,h\nu)dE, \quad (20)$$

where $Y(h\nu)$ is given in units of electrons photoemitted per absorbed photon.

From the above analysis, we see that the absolute quantum yield and the EDC's for primary photoelectrons can be expressed in terms of the ODS, $\alpha(h\nu)$, $L(E)$, and a $T_F(E)$ appropriate to a spherical conduction band.

In the interpretation and analysis of the experimental photoemission data, we shall find it necessary to know the value of $L(E)$. Since no experimental values of $L(E)$ are presently available, we shall calculate $L(E)$ from

[18] For a plot of the correction factor C, and for an alternative derivation of Eq. (17), see Refs. 1 and 15.

the ODS, using the relationship

$$L(E)=K|v_g(E)|\Big/\int_{E_F}^{2E_F-E}d(E_i^0)\int_{E_F-E_i^0}^{(E-E_i^0)/2}N_V(E_i^0)\times N_C(E-\Delta E)N_V(E_i^0+\Delta E)d(\Delta E)\,, \quad (21)$$

where K is an arbitrary constant and E_i^0 is the energy of the state from which the valence electrons are excited. Equation (21) has been derived earlier by Berglund and Spicer[1] and is based upon the simplifying assumption that the collision probability of a hot electron with a valence electron is determined solely by the number of valence electrons, the number of empty states in the conduction band, and conservation of energy. Note in Eq. (21) that, aside from the scale factor K, the value of $L(E)$ is determined solely by the ODS and the velocity of the hot electron.

In addition to being related to $L(E)$, the ODS is related to ϵ_{2b} (the "interband" or non-Drude contribution to the imaginary part of the dielectric constant) by the relationship[2]

$$\epsilon_{2b}(h\nu)=\frac{A}{\nu^2}\int_{E_F}^{E_F+h\nu}N_C(E)N_V(E-h\nu)dE, \quad (22)$$

where the factor A includes the square of the matrix element M.

IV. PROCEDURE FOR OBTAINING OPTICAL DENSITY OF STATES FROM PHOTOEMISSION AND OPTICAL DATA

From Eqs. (17), (20), and (21), we see that the ODS and the threshold function can be expressed in terms of the EDC's, the quantum yield, and the electron-electron scattering length, all of which are experimental observables. In addition, Eq. (22) relates the ODS to the shape of ϵ_{2b}, which is also an observable. In the analysis of our photoemission data, we have attempted to find an ODS that is quantitatively self-consistent with Eqs. (17) and (20)–(22). In doing so, the scale factor K in Eq. (21) must be determined. This is done in the present work by using the measured value of quantum yield at one photon energy. In addition, the bottom of the free-electron conduction band that determines the envelope of the conduction-band density of states must be located. This sets the threshold function $T_F(E)$ and the hot electron velocity $v_g(E)$. In applying Eq. (17), we have used published[14] experimental values for the absorption coefficient $\alpha(h\nu)$.

By use of the analysis and relationships described above, we have found an ODS for Cu that appears, within experimental error and within the accuracy of the analysis, to be remarkably self-consistent with the experimental observables in Eqs. (17) and (20)–(22). In Ref. 15 it is shown that if the $L(E)$ given by Eq. (21) is specified by even a single experimental point, then the self-consistent set $[N_V(E),N_C(E),T_F(E)]$ is unique. In the case of Cu, however, no experimental data are available for $L(E)$; consequently, we have in our calculations obtained $L(E)$ at one energy using the experimental value of yield and Eq. (20). We will discuss $L(E)$ in detail in Sec. VI.

The following process was used to obtain a self-consistent ODS:

(a) The energy locations of peaks in the valence bands were deduced from peaks in the experimental EDC's that behave in the manner of nondirect transitions, and the locations of peaks in the conduction band were deduced from stationary peaks in the EDC's. The one peak in the experimental EDC's that showed a definite direct-transition nature[2] was ignored in the nondirect analysis.

(b) As a first approximation, the shape of the valence-band density of states was chosen to be very similar to the shape of the experimental EDC's at energies a few eV above threshold. Since the escape probability is almost constant in this energy region, the EDC's should closely approximate the escape probability. Relatively minor adjustments of peak heights were then made for best agreement with all observables.

(c) The shape of the conduction band was determined by arbitrarily adjusting the location of the bottom of the free-electron band and superimposing conduction-band structure upon this free-electron envelope. The relative peak heights of the conduction-band structure were chosen to obtain the best over-all agreement with experimental observables.

(d) $L(E)$ was normalized at $\sim$8 eV to give good agreement with the experimental EDC's and quantum yield as outlined above.

(e) The scale factor A of Eq. (22) was chosen so as to compare the shape of the calculated ϵ_{2b} with the experimental ϵ_{2b}.

Having obtained a first approximation to the ODS and a normalization point for $L(E)$, Eqs. (17) and (20)–(22) were evaluated for many different photon energies with the use of the Burroughs B5500 computer, and the results were compared with experiment. The ODS as well as the adjustable parameters were then modified in an attempt to improve the agreement between theory and experiment. Finally, the cycle was repeated. In practice, only a small number of iterations was necessary before self-consistency was achieved and the change in parameters from that chosen originally was found to be small.

V. OPTICAL DENSITY OF STATES OF COPPER

In the last two sections we described how an ODS could be obtained which would be consistent with all of the available experimental data. In this section we shall present and discuss the ODS derived for Cu. In Sec. VI we will present the experimental data and compare

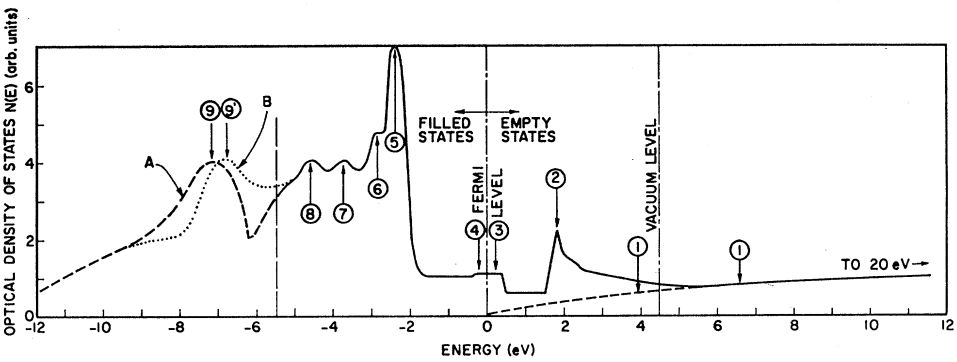

FIG. 4. ODS states for Cu, extending from ~ -11 to $\sim +20$ eV above the Fermi level. The numbered arrows indicate structure which will be discussed in the text. The curve below -5 eV is dashed because this is determined with less accuracy than that at higher energy. Curves A and B in this region indicate two possible ODS curves.

them to the results calculated on the basis of the ODS and the nondirect model presented in Sec. IV.

The ODS that has been deduced from experimental photoemission and optical data is shown in Fig. 4. In the valence band the locations of the peaks labeled 5–8 have been obtained from our new photoemission data on clean Cu, and the location of peaks 4, 9, and 9′ have been obtained from earlier data[2] on cesiated Cu. The location of peaks 4–8 is probably accurate to within ± 0.1 eV, and the location of peak 9′ is probably accurate to within about ± 0.3 eV. On the basis of our original calculations (which consider only primary electrons) the location and strength of peak 9 was chosen to give agreement with the cesiated Cu data. However, the lower portions of the cesiated EDC's for photon energies greater than about 8 eV are almost completely dominated by secondary (scattered) electrons, so that the location and strength of peak 9 could not be well ascertained by the present analysis. Fortunately, Eastman[19] has very recently analyzed the photoemission data by including in his analysis scattered (secondary) electrons in the manner of Berglund and Spicer[2]; he finds that our peak 9 does not result in complete EDC's (primary plus secondary electrons) which agree well at high photon energies with experimental EDC's for cesiated Cu. However, using Eastman's calculations, we find that if peak 9 is displaced and slightly reshaped, the resulting peak 9′ is in excellent agreement with the cesiated copper EDC's; consequently, we feel that peak 9′ and ODS B is more correct than peak 9 and ODS A. However, because the difference between ODS A and ODS B is so slight, the use of ODS B gives essentially the same results as the use of ODS A, except in the detailed shapes of high photon energy EDC's. Therefore, we have revised our calculations only where there is a significant effect, and most of the calculations presented in this paper are based upon ODS A.

In the conduction band, the bottom of the free-electron-like conduction band is located at the Fermi level, and envelope 1 of the conduction band has a $\sqrt{E}$ energy dependence. The large sharp peak 2 is taken from the cesiated Cu data of Berglund and Spicer.[2] In their data, this peak is clearly seen at an energy only a few tenths of 1 eV above the vacuum level. Since only a very strong peak is likely to be seen so near the vacuum level (1.6 eV in cesiated Cu), the strength attributed to peak 2 seems justified. In the analysis used to determine the ODS, the magnitude of the entire conduction-band density of states can be scaled by the same arbitrary constant without affecting any of the results. In Fig. 4 the conduction-band density of states is scaled to match the valence-band density of states at the Fermi level.

The vacuum level of 4.5 eV shown in Fig. 4 is the vacuum level appropriate to our data on clean Cu. This vacuum level was found to vary by several tenths of 1 eV from sample to sample, but with no effect on the structure in the experimental EDC's. This variation in vacuum level may be due to different crystal faces being exposed in different evaporated films.

With regard to the conduction-band density of states, the greatest uncertainty lies in the region between the Fermi level and ~ 1.6 eV above the Fermi level, since this region cannot be directly investigated by photoemission. Here we depend principally on a fit with ϵ_2. (This will be discussed in more detail in Sec. VIII.) In addition, it is difficult to determine the detailed nature of the valence band for energies lower than ~ 8 eV below the Fermi level, but the conclusion can be made that $N_V(E)$ is quite small in this energy range. The over-all uncertainty in the shape of the valence band (with peak 9′), $\Delta N_V(E)$, is crudely estimated to be

$$\Delta N_V(E) \cong (|E|/20) N_V(E) \quad \text{for} \quad E<0 \text{ eV}, \quad (23)$$

where the zero of energy is taken at the Fermi level. Consequently, if $N_V(E)$ is pegged at the Fermi level, then the relative uncertainty in the height of peak 9′ is, roughly, $\pm 33\%$.

Another uncertainty in Fig. 4 is the location of the bottom of the free-electron band; it was found that by moving the bottom of the free-electron band by as

[19] D. Eastman (private communication).

much as ±1 eV about the Fermi level, and by making appropriate small adjustments in other parameters, nearly as good a fit with the experimental data could be achieved. However, excursions of more than about ±1 eV resulted in poorer over-all fits with the experimental observables, owing mainly to the fact that near threshold the shape of the threshold function $T_F(E)$ is quite sensitive to the location of the bottom of the free-electron band [as can be seen from Eq. (18)].

Note that in the region between −2 and −6 eV below the Fermi level, $N_V(E)$ is significantly different from the earlier density of states shown in Fig. 16 of Ref. 2. We believe that our present improved result is a direct consequence of the extreme care that we have taken with regard to vacuum conditions and to the elimination of any possible surface contamination during the preparation and testing of the copper films. It is also recognized that the cesium monolayer used by Berglund and Spicer[2] may have affected their ODS.

VI. ELECTRON-ELECTRON SCATTERING LENGTH AND EFFECTIVE THRESHOLD FUNCTION

The electron-electron scattering length calculated from Eq. (21) using density of states A of Fig. 4 is plotted in Fig. 5. Here $L(E)$ has been taken as 22 Å at 8.6 eV above the Fermi level to give the best agreement between the calculated and measured quantum yields. This $L(E)$ is virtually indistinguishable from the $L(E)$ that would be calculated from ODS B, owing to the smoothing nature of Eq. (21).

One would like to compare the $L(E)$ determined here with that determined in a different experiment. Since appropriate data are not available for Cu, we will make the comparison with Au. Because of the smoothing nature of Eq. (21), the shape of $L(E)$ is insensitive to all but the most gross features of the density of states. Since the gold and copper d states lie at almost the same depth below the Fermi level, and since other features such as the s, p, and d configurations are similar for these two noble metals, one might expect the Cu and Au ODS—and thus $L(E)$—to be grossly similar. We have studied gold and found this to be the case.[15,20] In Fig. 5 we include the experimental points of Kanter[21] for Au. As can be seen, agreement both for shape and magnitude is good. Reasonable agreement has also been obtained between our $L(E)$ and Kanter's $L(E)$ for Au. This good agreement gives added confidence in the analysis of our data and in the assumptions which have gone into the analysis. The theoretical work of Kane[22] on electron-electron scattering gives added support to the assumptions used in calculating $L(E)$.

At energies greater than ~10 eV above the Fermi level, $L(E)$ is less than 20 Å, indicating that at these high energies the bulk of the photoemitted electrons come from within a few atomic layers of the surface. However, the experimental EDC's from clean Cu do not seem to show any drastic anomalies at high photon energies, indicating that electrons originating from very near the surface still exhibit bulk properties. However, the broadening observed at high energy may be due to some smearing of the electronic structure near the surface. As seen from Eq. (17), the probability of escape is not determined solely by the free-electron threshold function $T_F(E)$, but by the effective threshold function

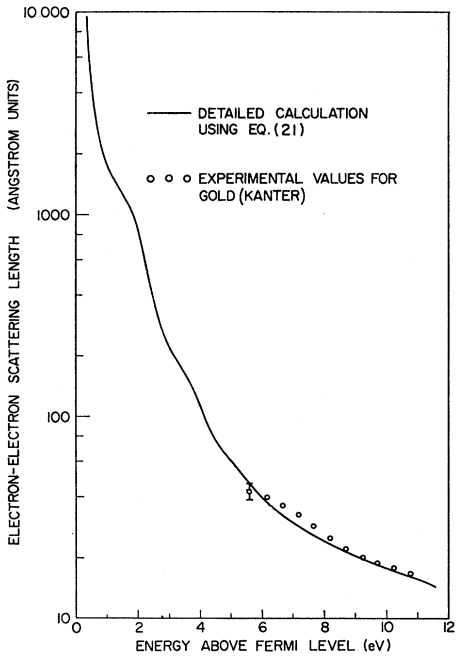

FIG. 5. Calculated electron-electron scattering length $L(E)$ for Cu. The magnitude of $L(E)$ was set equal to 22 Å at 8.6 eV to give experimental photoemission yield. The experimental points are from an independent experiment by Kanter on Au (see Ref. 21).

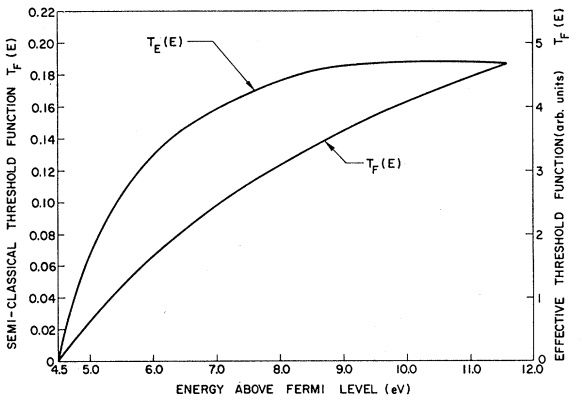

FIG. 6. Comparison of semiclassical threshold $T_E(E)$ to effective threshold function $T_F(E)$ for copper. $T_F(E)$ was obtained by taking into account the electron-electron scattering length of Fig. 5.

[20] W. F. Krolikowski and W. E. Spicer (unpublished).
[21] H. Kanter (unpublished).
[22] E. O. Kane, Phys. Rev. **163**, 1544 (1967).

$T_F(E)$, which is affected by $L(E)$. Once $L(E)$ is available, $T_F(E)$ can be calculated. In Fig. 6 we have plotted the $T_F(E)$ for clean Cu that applies in the range of photon energies 7.7–11.6 eV, and compared the shape of $T_F(E)$ with $T_F(E)$. As will be seen in Fig. 15, $T_F(E)$ is nearly constant in the range ~6.5–11.6 eV above the Fermi level, thus enhancing the resemblance between the EDC's and the valence-band density of states, since above 6.5 eV there is no structure in the conduction-band density of states.

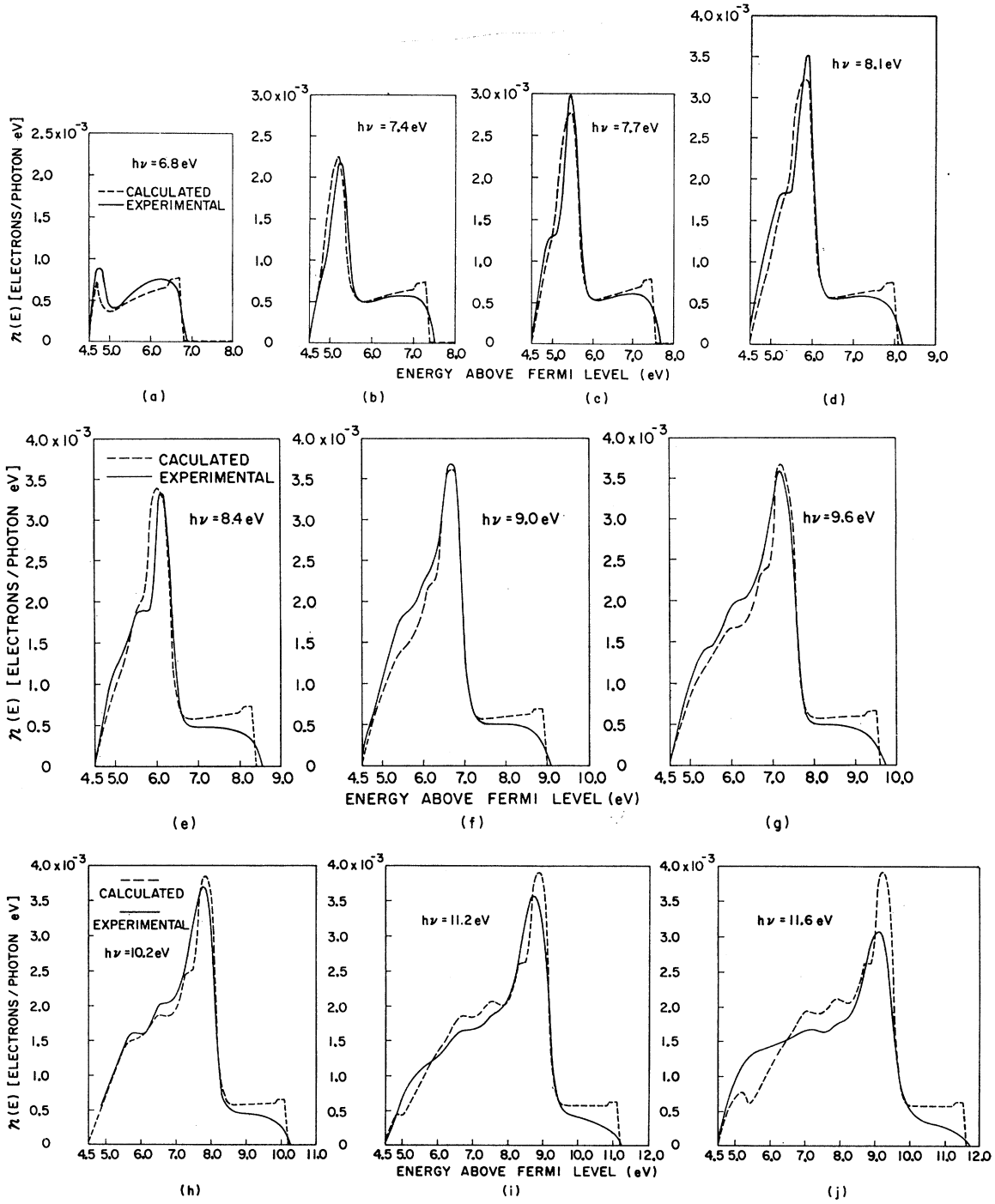

FIG. 7. Calculated and experimental EDC's for clean Cu. Note that both the calculated and experimental EDC's are plotted against the same vertical scale, so that the comparison is on an absolute basis.

VII. CALCULATED AND MEASURED ENERGY-DISTRIBUTION AND YIELD CURVES

A. Photoemission from Clean Copper

In Fig. 7 typical experimental EDC's from our measurements on clean Cu are compared with calculated EDC's over the range of photon energies 6.8–11.2 eV. The EDC's were calculated using the ODS A of Fig. 4, Eq. (17), and the $L(E)$ of Fig. 5. Note that in the experimental data there is almost no evidence of secondary (scattered) electrons even for photon energies up to 11.6 eV. It is very important to recognize the striking similarity between the structure in the EDC's and the structure in the d-band density of states. Parameters such as $L(E)$ are more important in determining the absolute magnitude of the EDC's than in determining the structure in them.

In Fig. 8 we compare our experimental EDC at $h\nu = 10.2$ eV with the corresponding experimental EDC of Vehse and Arakawa,[6] where over-all agreement with regard to both shape and magnitude is fair. However, our EDC's exhibit more fine structure and do not have the pronounced low-energy shoulder seen in Vehse and Arakawa's EDC. Such a low-energy shoulder is evident in all of Vehse and Arakawa's EDC's in Figs. 8 and 9 and is possibly due to very slight contamination of the Cu surface, since their work was done in a windowless system at a pressure of about 3×10^{-8} Torr. Vehse and Arakawa have obtained relatively high quality EDC's at photon energies to 20.4 eV, and we present these EDC's in Fig. 9. At our request, Eastman[19] has kindly calculated the corresponding EDC's (including primaries and secondaries) to be expected from our copper ODS (Fig. 4); his results are compared with experiment in Fig. 9. Note that the secondary electrons are not important for photon energies less than 12 eV, but dominate the low-energy part of the EDC's for photon energies greater than ~14 eV. From peak 9 of Fig. 9 we can see that the use of ODS B gives slightly better agreement than the use of ODS A. As can be seen from Figs. 7–9, the agreement between the calculated and experimental EDC's on clean Cu is good with respect to both the shape and magnitude of our EDC's and the EDC's of Vehse and Arakawa. Experimental justification for the valence-band peaks 5–8 of Fig. 4 is indicated in Fig. 7 and for peak 9′ in Fig. 9. In Fig. 7(d) we see evidence that peak 5 has tremendous strength, yet can be resolved by our photoemission measurements to have a half-width of only ~0.5 eV. At photon energies greater than ~9.5 eV, the small peak 6 merges as a shoulder on peak 5 and can no longer be resolved. This loss in resolution may be due to lifetime broadening, as discussed earlier in Ref. 2, or to photoexcitation very near the surface.

In Fig. 10 the experimental quantum yield is compared to the yield calculated from Eq. (20). The inflection point in the quantum yield at a photon energy of ~6.5 eV is due to the onset of photoemission from the very strong valence-band peak 5. Over the entire range

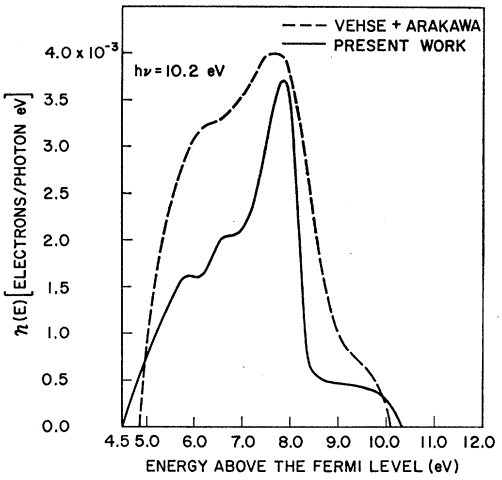

FIG. 8. Comparison of experimental EDC's of Cu at $h\nu = 10.2$ eV. The dashed curve is taken from the work of Vehse and Arakawa (Ref. 6) and the solid curve is taken from the present work. Both curves are on the same absolute scale.

of photon energies 5–11.6 eV, we see that the calculated and experimental quantum yields are in excellent agreement.

The effect of inadequate vacuum conditions on the copper EDC's is dramatically demonstrated in Fig. 11, where it is seen that the EDC's from contaminated Cu are characterized by a large peak of slow electrons which did not move with photon energy and by loss of fine structure. In this case, the large low-energy peak of electrons cannot be associated solely with an increase in the inelastic scattering probability since there is no corresponding loss of high-energy electrons. Similar results have been obtained by Vehse and Arakawa.[6] More work must be done before this contamination effect can be understood in detail.

As an aside, it should be noted that this contamination effect is considerably different from that observed in Ni.[7] For Cu, a new peak appears near the low-energy cutoff. Its magnitude grows with $h\nu$, but its position does not move. In Ni, however, the peak moved to higher energy as $h\nu$ increased.

B. Photoemission from Cesiated Copper

If our model for the photoemission process and the ODS is correct, then we should be able to obtain agreement between calculations and experiment for the case of cesiated Cu, provided that cesiated Cu differs from clean Cu only in the reduction of the work function. Consequently, we have calculated the quantum yield and EDC's for cesiated Cu using exactly the same method of analysis described earlier in this paper—except that the work function was changed from 4.5 to 1.6 eV; representative results are shown in Figs. 12–14, where our present calculations are compared with the earlier data of Ref. 2 on cesiated Cu.

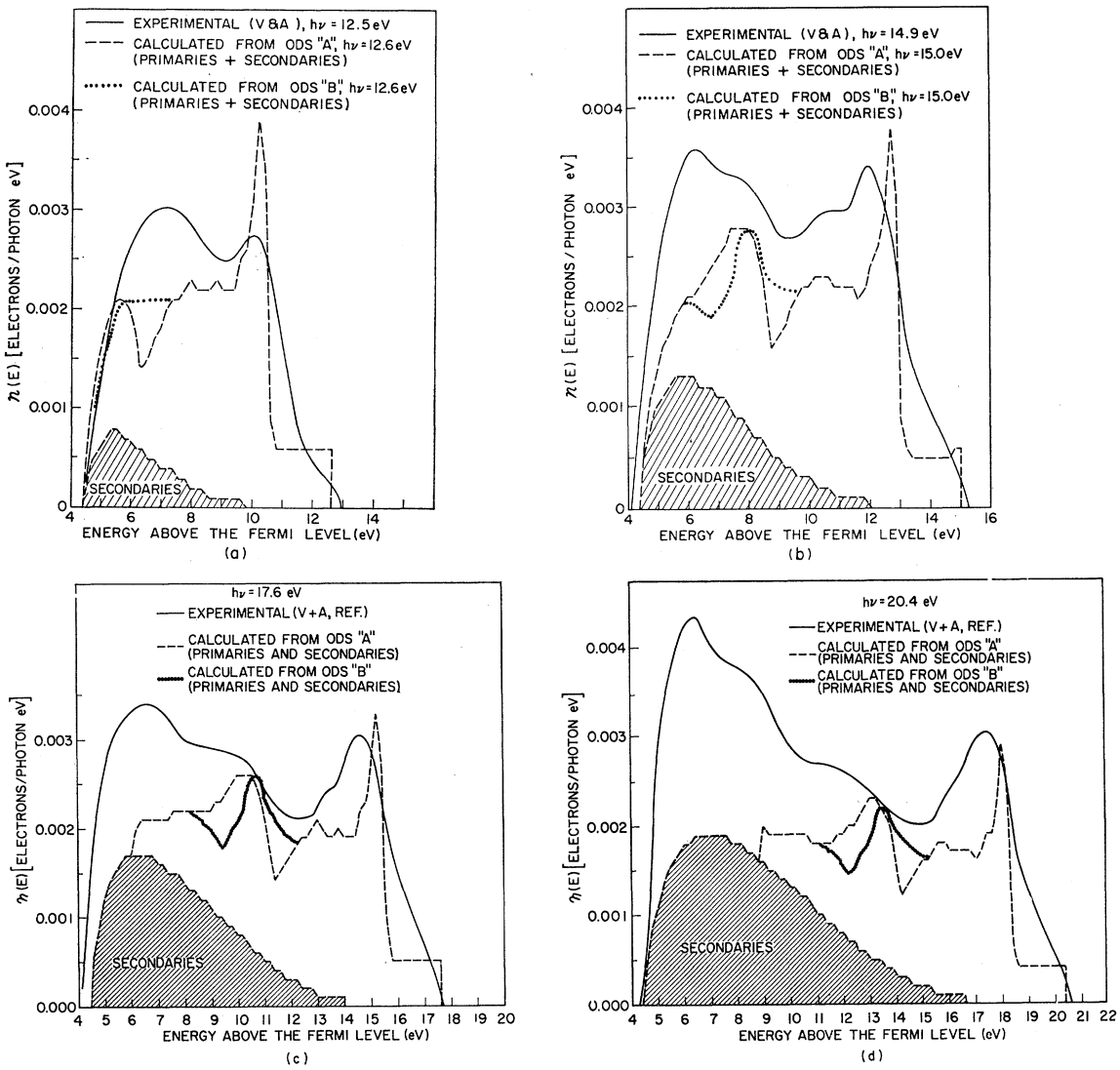

FIG. 9. Comparison of the experimental EDC's of Vehse and Arakawa (Ref. 6) from clean Cu with the EDC's calculated in this work. The experimental EDC's have been normalized to the experimental yield of Vehse and Arakawa, and the calculations from ODS A have been done by Eastman for a work function of 4.4 eV and the $L(E)$ of Fig. 6.

As seen from Fig. 12, the magnitudes of the calculated and experimental yields are in fairly good agreement just above the vacuum level and in the range of photon energies 4–11.6 eV. However, there is a glaring discrepancy between 2 and 4 eV, in that the experimental curve shows a large dip that is not predicted by the calculation. Strangely enough, the *shapes* of the calculated and experimental EDC's in this range of photon energies are in good agreement, as seen from Figs. 13(a) and 13(b). At the present time, we can only speculate on the cause of this discrepancy, which may be due to such causes as electron-phonon scattering, inappropriateness of the free-electron model in calculating transport effects and the threshold function, and possible Cu-Cs interaction. It is also possible that the early yield measurements were inaccurate.

In Fig. 13(c) the peak which appears in the experimental EDC at ~4.2 eV has been previously[2] identified as a direction transition near L; therefore, one would not expect to see the peak in the calculated curve, since it is based on nondirect transitions only. It should be noted that the direct transition accounts for only about 7% of the photoemitted electrons.

At higher photon energies, we see in Figs. 13(c) and 13(d) that theory and experiment appear to be in good qualitative agreement, especially if one is not too critical in accounting for the missing scattered electrons which were not included in the calculations in Fig. 13(d), which is for a photon energy of 10.4 eV.

For photon energies greater than ~8 eV, one is able to distinguish between density-of-states models A and B of Fig. 4 by comparing the cesiated copper EDC's with calculations that include both primary and secondary electrons. Eastman[19] has performed these calcula-

tions and has found that Fig. 13(d) (which is based upon density of states A and only a primary-electron calculation) is deceptive, in that, when secondary electrons are included, peak 9 in ODS A results in a predicted shoulder at $\sim$2.7 eV above the Fermi level, whereas the experimental shoulder is observed at 3.3 eV, as shown in Fig. 14(a). The discrepancy is even more apparent in Fig. 14(b), where the experimental shoulder is at $\sim$4.1 and the calculated shoulder at $\sim$3 eV. As seen in both Figs. 14(a) and 14(b), ODS B results in excellent agreement with experiment, even though ODS B is only slightly different from ODS A. This occurs because secondary electrons dominate in the vicinity of the shoulder, with the result that the location of the calculated shoulder is extremely sensitive to the detailed shape of peak 9 in the ODS. As seen from Fig. 14, the agreement between the calculated and experimental EDC's is good with regard to both shape and magnitude for cesiated Cu at high photon energies, if secondary electrons are accounted for in the calculations.

VIII. OPTICAL CONSTANT ϵ_{2b}

The shape of the ϵ_{2b} calculated using Eq. (22) and ODS A of Fig. 4 is shown in Fig. 15(a), where three distinct pieces of structure can be seen. Owing to the smoothing nature of Eq. (22), the ϵ_{2b} calculated from ODS A is almost identical to the ϵ_{2b} calculated from ODS B. The identification of the initial and final states for this structure is presented in Table I. Various authors[14,23–26] have obtained experimental values of ϵ_{2b} from reflectivity measurements; unfortunately, their results are not consistent in detail, so we do not have at the present time a definitive experimental ϵ_{2b} with which to compare our calculated ϵ_{2b}. However, the general features of all the available experimental curves are es-

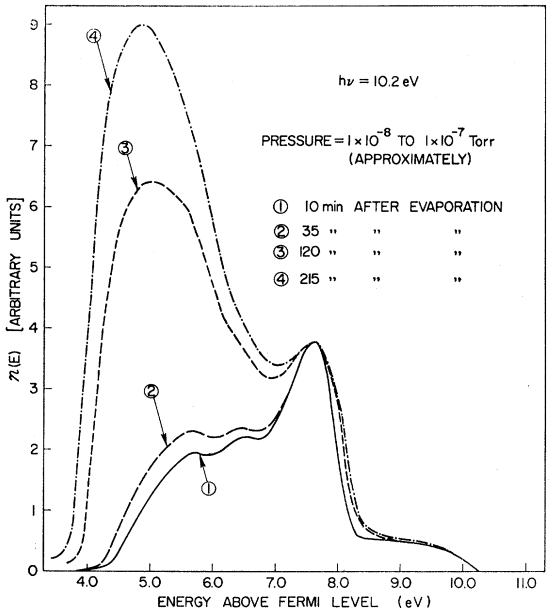

FIG. 11. Effect of inadequate vacuum on copper energy-distribution curves. These curves were *not* fitted, and the relative magnitudes were experimentally observed. Note that the peak at 7.6 eV above the Fermi level did not change magnitude with time.

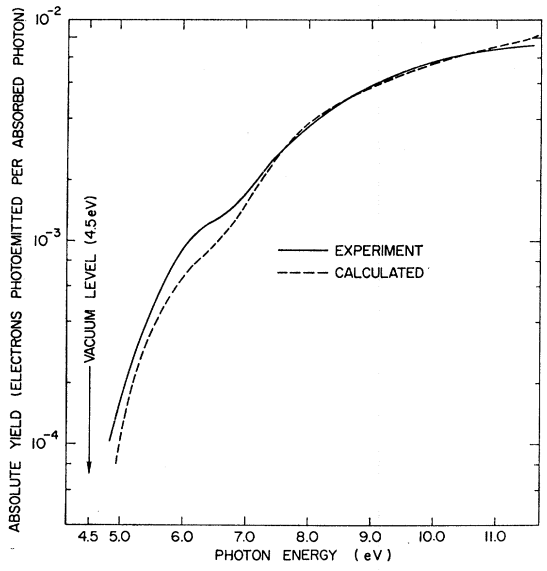

FIG. 10. Comparison of experimental and calculated yields for Cu. The calculated yield was obtained using ODS A of Fig. 4 and $L(E)$ of Fig. 5.

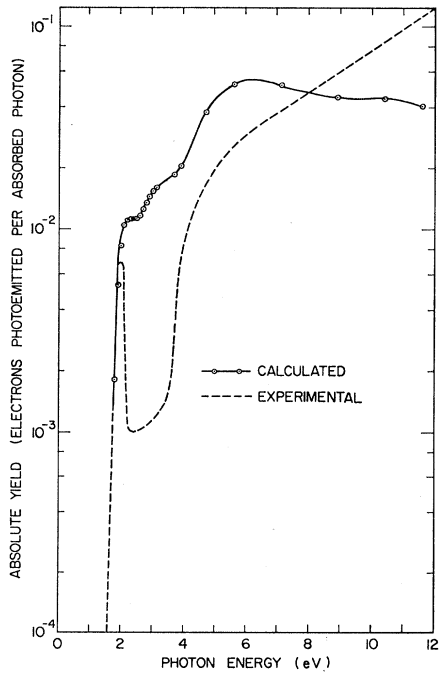

FIG. 12. Comparison of calculated and experimental (Ref. 2) photoelectric yields for Cu with a surface monolayer of Cs.

[23] B. R. Cooper, H. Ehrenreich, and H. R. Philipp, Phys. Rev. 138, A494 (1965).
[24] D. Beaglehole, Proc. Phys. Soc. (London) 85, 1007 (1965).
[25] M. Garfinkel, J. J. Tiemann, and W. E. Engeler, Phys. Rev. 148, 695 (1966).
[26] U. Gerhardt, Phys. Rev. 172, 651 (1968).

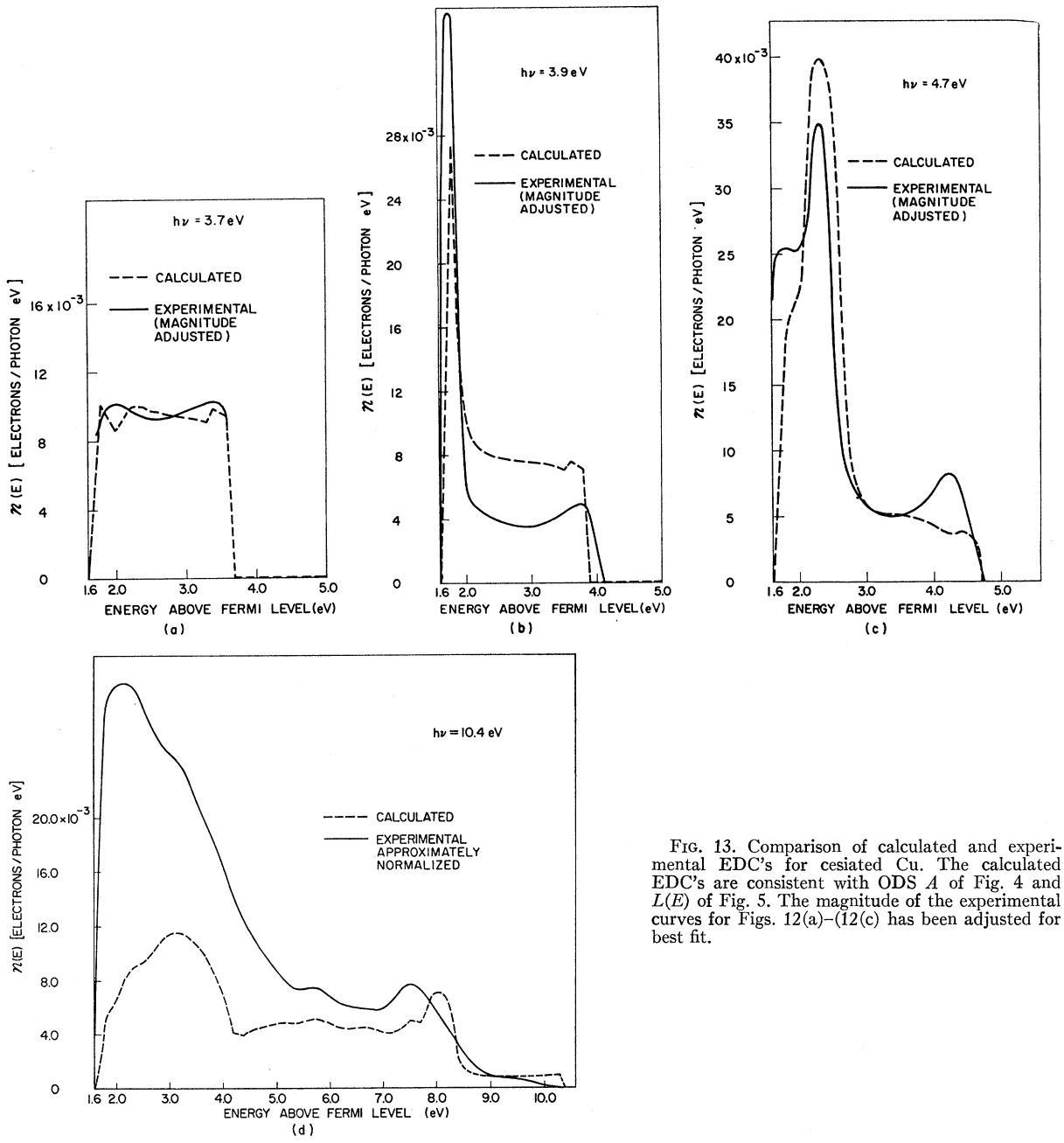

FIG. 13. Comparison of calculated and experimental EDC's for cesiated Cu. The calculated EDC's are consistent with ODS A of Fig. 4 and $L(E)$ of Fig. 5. The magnitude of the experimental curves for Figs. 12(a)–(12(c) has been adjusted for best fit.

sentially the same; thus, we have compared our calculated ϵ_{2b} with the experimental data of two different authors[14,24] in Figs. 15(b) and 15(c). As seen from these figures, the agreement between the calculations and experiment is reasonable. The only major disagreement lies in the location of peak C, which our calculation predicts to be at 4.2 eV and experiment finds to be at ~4.7 eV. The location of peak C in the calculated ϵ_{2b} is determined largely by the location of peak 2 in the conduction-band density of states, which was experimentally found by Berglund and Spicer[2] to occur at 1.8 eV above the Fermi level, since in their experimental EDC's a pronounced fixed peak appeared at ~0.2 eV above the vacuum level of ~1.6 eV. There is also disagreement in the steepness of the high-energy edge of peak C. Experimentally this edge is found to be much steeper than the calculations indicate. It should be noted that, if the ODS were cut off at about 5.5 eV, better agreement would result.

Not included in the nondirect calculation of ϵ_2 presented in Fig. 15 are contributions from direct transitions. There is a well-established[2,26] direct transition due to states near the L point of the zone which contributes optical strength for $h\nu > 4.2$ eV. Addition of this to the

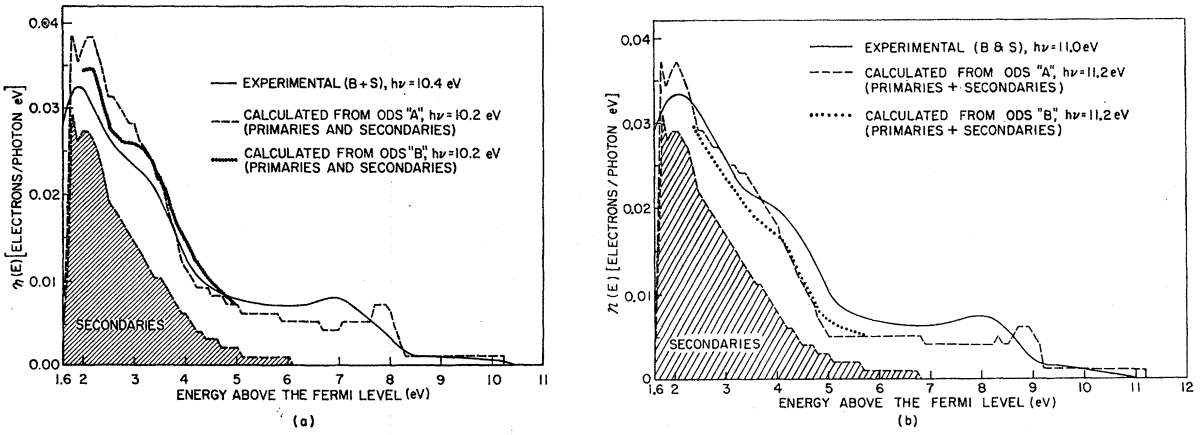

FIG. 14. Comparison of experimental EDC's from cesiated Cu (Ref. 2) with the calculated EDC's, including both primaries and secondaries. The calculations from ODS *A* were done by Eastman (Ref. 11). The experimental EDC's were normalized to the experimental yield (Ref. 2). The small "dip" at about 1.8 eV is an artifice of the calculation and has no physical significance.

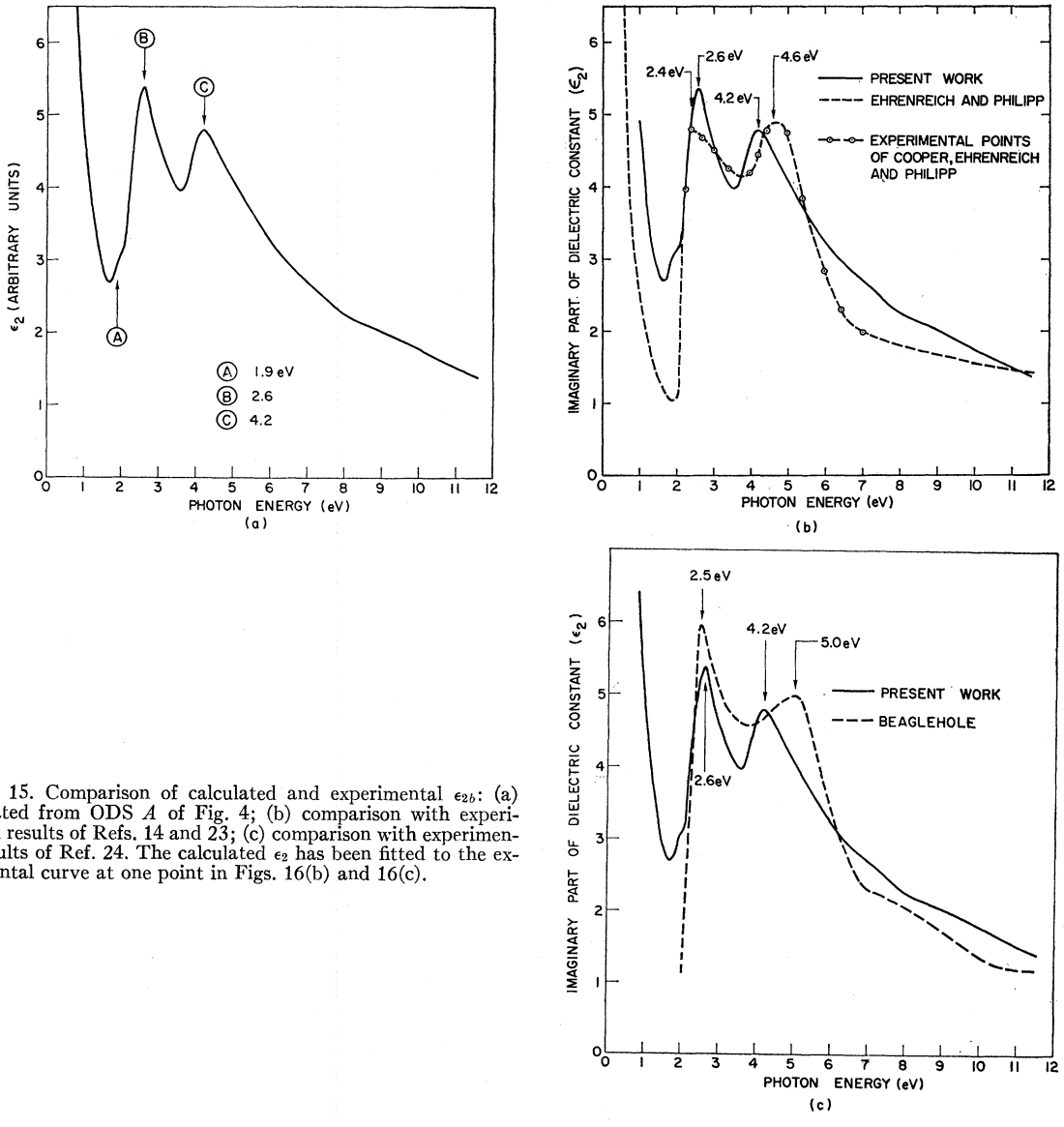

FIG. 15. Comparison of calculated and experimental ϵ_{2b}: (a) calculated from ODS *A* of Fig. 4; (b) comparison with experimental results of Refs. 14 and 23; (c) comparison with experimental results of Ref. 24. The calculated ϵ_2 has been fitted to the experimental curve at one point in Figs. 16(b) and 16(c).

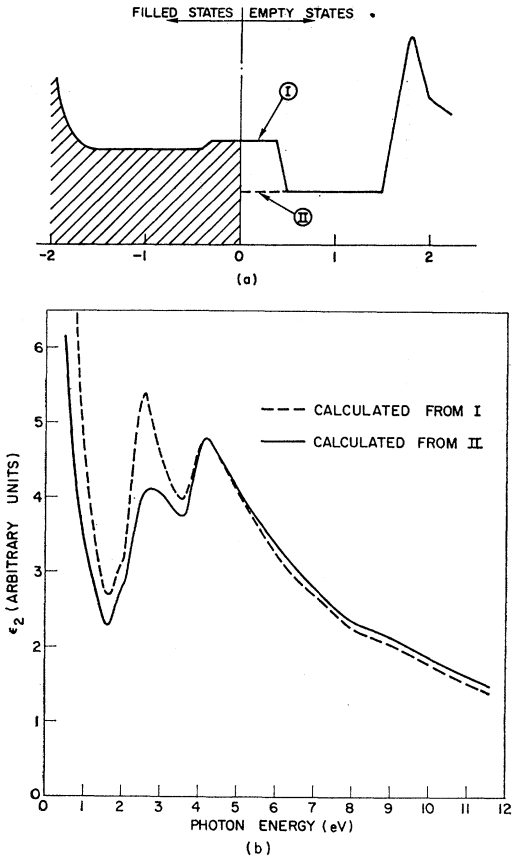

FIG. 16. Effects of different ODS on the calculated ϵ_2: (a) different ODS used to calculate ϵ_2 for Cu (see Fig. 4); (b) comparison of shapes of ϵ_2 calculated from density of states I and from density of states II of Fig. 16(a).

nondirect transition would improve the agreement with experiment.

Since we do not have any direct experimental data to characterize the region between the Fermi level and $\sim$1.6 eV above the Fermi level, there is a certain degree of arbitrariness in the manner in which we have estimated the ODS in this region. Because of their integral character, our results for ϵ_{2b} are not sensitive to the detailed nature of the density of states just above the Fermi level. This is demonstrated in Fig. 16, where the complete removal of conduction-band "peak" 3 serves only to reduce somewhat the strength of peak B in ϵ_{2b}. At the present time, the published experimental values vary considerably in the relative strength of peak B, so that we are unable to determine which ODS in Fig. 16(a) are more appropriate.

TABLE I. Identification of structure in calculated ϵ_{2b} of Fig. 16(a).

Peak in ϵ_{2b} [Fig. 16(a)]	Initial valence-band state (Fig. 4)	Final conduction-band state (Fig. 4)
A: 1.9 eV	4	2
B: 2.6 eV	5	3
C: 4.2 eV	5	2

The reader may have noted that although our present valence-band density of states differs significantly from the earlier valence-band density of states of Berglund and Spicer,[2] their earlier work resulted in a calculated ϵ_{2b} that is in somewhat better agreement with experiment than the present calculation shown in Fig. 16. However, there was apparently a serious error in their ϵ_{2b}, and the excellent agreement between the calculated and the experimental ϵ_{2b} in Fig. 27 of Ref. 2 is erroneous. Nevertheless, it must be emphasized that the conclusions of Ref. 2 are not incorrect, but appear to be entirely consistent with the present work.

IX. COMPARISON OF OPTICAL DENSITY OF STATES WITH DENSITY OF STATES OBTAINED BY OTHER METHODS

A. Comparison with Calculated Density of States

In Figs. 17 and 18 we compare the ODS with that obtained from band calculations. In Fig. 17 the comparison is with a calculation by Snow,[27] who used an APW calculation with an exchange potential proportional to $\frac{5}{6}\rho^{1/3}$. Snow performed several calculations with different coefficients in front of the $\rho^{1/3}$ term to obtain the best fit with the experimental data. The d- to Fermi-level separation was sensitive to this coefficient; however, the fit was not perfect. In order to make the fit as good as possible, Snow's density of states was shifted by 0.2 eV to bring the calculated and measured d states to Fermi-level energy in exact agreement. The comparison in Fig. 18 is with the calculation of Cohen and Mueller.[28] Above -5 eV there are four principal pieces of structure

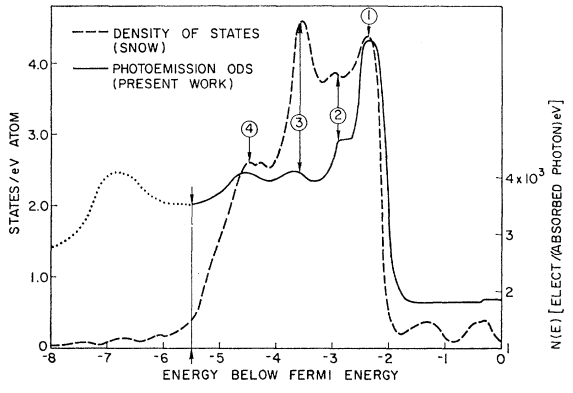

FIG. 17. Comparison of the ODS with the density of states calculated by Snow (Ref. 27) using an $\frac{5}{6}\rho^{1/3}$ exchange term. Snow's density of states has been shifted by 0.2 eV to place the Fermi-level–to–d-band energy in exact agreement with experiment. The absolute scale was placed on the ODS by placing eleven electrons between the Fermi level and -5.5 eV. Note that the four pieces of numbered structure coincide rather well in energy.

[27] F. C. Snow, Phys. Rev. **171**, 785 (1968).

[28] M. H. Cohen and F. M. Mueller, in *Atomic and Electric Structure of Metals* (American Society of Metals, Metals Park, Ohio, 1967), p. 75.

in each density of states labeled 1–4, although the relative heights of these vary considerably in the three curves; the positions in energy of the structure coincide within a few tenths of 1 eV. It is encouraging that the two band calculations done by such different methods yield similar position in energy of the structure. It is also striking that the structure in the ODS lines up so well with the structure in the calculated density of states. This suggests that the ODS above −5 eV may be closely related to the density of states obtained from band calculations. In both the band calculation and the experimental determination of the ODS, it is much easier to determine the position in energy of a piece of structure than to determine accurately its relative amplitude. In addition, there is a question as to whether the matrix elements which must enter into the ODS are independent of initial-state energy. If they are not, the peak heights in the optical density will not necessarily reflect the true state density (see Secs. I, III, and IV). Thus, it is not surprising that there is a difference in peak height even though the peak positions coincide rather well.

Up to this point, we have ignored the lowest-lying peak in the ODS (peak 9′). This occurs at ∼6.8 eV below the Fermi level. It is dotted in Figs. 4, 17, and 18, since it is much more difficult to determine experimentally than is the higher-lying ODS. Based on the relatively good agreement between ODS and calculated band structure at higher energy and on the strong disagreement below 5.5 eV, we would venture to guess that the strong 6.8-eV peak is not an accurate reflection of a strong peak in the ground-state density of states. Rather, it seems likely due to some other phenomena—perhaps a simultaneous plasmon and one-electron excitation as suggested by Nesbet and Grant.[29] However, possible matrix-elements[30] or other effects[31,32] also cannot be ruled out at this time. Before speculating further on the origin of this peak, additional experimental work should be done. Of particular interest would be ultra-high-vacuum work (pressure $<10^{-9}$ Torr) for $h\nu>12$ eV, so that one could study the ODS for energies more than 5 eV below the Fermi surfaces in clean Cu under the best possible vacuum conditions.

In Figs. 17 and 18, the ODS have been put on an absolute basis by integrating under the ODS curve and assigning eleven electrons to the states below the vacuum level. In view of the discussion in the preceding paragraph, the ODS was taken to be zero below −5.5 eV in doing this. If the complete ODS curve below −5.5 eV were used, it would decrease the density of states by a factor of 0.56.

Another point of interest is the relative height of the density of states between the top of the d states and the Fermi surface, i.e., in the energy region where the states are derived strongly from atomic s and p states rather than d states. In this region, the ODS on the average is several times higher than the density of states obtained from band calculations. This would appear to be due to a stronger matrix element for transitions from the almost free-electron-like s- and p-derived states[33] than for transitions from the d-derived states.

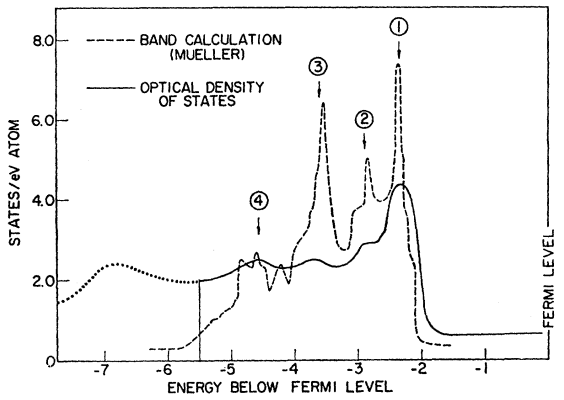

FIG. 18. Comparison of the ODS with the density of states calculated by Mueller (Ref. 28). Note that the four groups of structure numbered 1–4 line up in energy.

B. Comparison with Results of Ion-Neutralization Spectroscopy

In Fig. 19 the ODS for Cu is compared to the density of states obtained by Hagstrum[34] from Cu via the ion-neutralization-spectroscopy (INS) technique which he has developed. The peak between −2 and −4 eV is associated with the d states. As can be seen, the width of this peak is considerably greater than the d width indicated by the ODS or calculated band structure. In addition, there is no detailed structure in the ion-neutraliza-

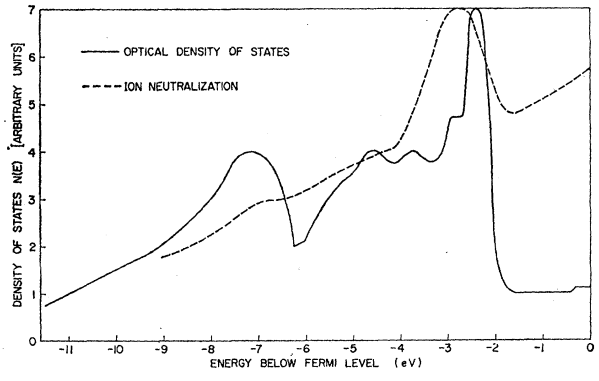

FIG. 19. Comparison between the ODS and the results obtained by Hagstrum (Ref. 35) through ion-neutralization studies.

[29] R. K. Nesbet and P. M. Grant, Phys. Rev. Letters **19**, 222 (1967).
[30] J. R. Cuthill, A. J. McAlister, M. L. Williams, and R. E. Watson, Phys. Rev. **164**, 1006 (1967).
[31] For other possibilities, see the discussion in Ref. 32.
[32] A. Yu-C. Yu and W. E. Spicer, Phys. Rev. **167**, 674 (1968).
[33] It is recognized that there is strong d admixture in these states as there is some s and p admixture in the "d-derived states." The present terminology is used simply for convenience.
[34] H. P. Hagstrum, Phys. Rev. **150**, 495 (1966).

tion results even though the instrumental resolution[34,35] is sufficient to resolve structure such as that seen in the ODS or calculated density of states. Hagstrum has noted[35] that, since his technique depends on electrons tunneling from the surface of the metal, it is sensitive to the electronic structure just at the surface and that, for d electrons, this structure may be different from that in the bulk of the material.

Even though the INS results suggest that the electronic structure just at the surface may be measurably different from that in the bulk of the material, the photoemission results indicate that the electronic structure within 10 or 20 Å of the surface is little changed from the bulk structure (see Secs. VI and VII A and Ref. 8).

C. Comparison with Results of X-Ray Photoemission Spectroscopy

The ODS for Cu is compared in Fig. 20 with the results obtained by Fadley and Shirley,[36] using the technique of x-ray photoemission spectroscopy (XPS). The XPS result is characterized by a single, almost symmetric peak with a width at half-maximum of ~3 eV. Since the total instrumental linewidth was ~1.0 eV, this width and lack of detailed structure do not appear to be instrumental. If we make the reasonable assumption that the broad peak is due to d electrons, it is also significant that there is little evidence for the s- and p-derived states lying within 2 eV of the Fermi surface (see Figs. 2, 17, and 18). These dates can be clearly seen in the photoemission and INS work. The lack of any detailed structure in the excitation from the d states would also seem to be significant, since such detailed structure does appear in the ODS as well as in the calculated band structure. However, it should be noted that substructure has been obtained in XPS results[36,37]

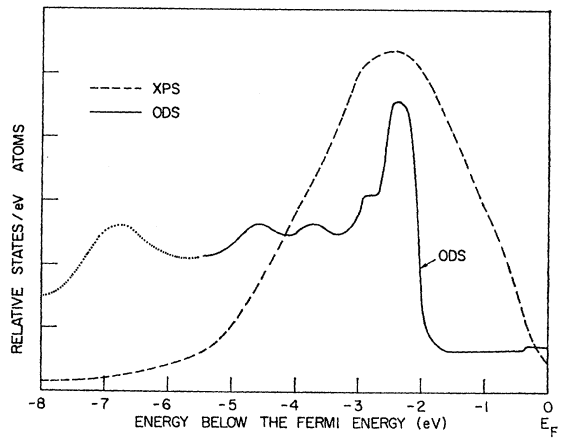

FIG. 20. Comparison between ODS and results of the x-ray photoemission (XPS) experiment of Fadley and Shirley (Ref. 36).

[35] H. P. Hagstrum (private communication).

[36] C. S. Fadley and D. A. Shirley, Phys. Rev. Letters **21**, 980 (1968).

[37] K. Siegbahn, C. Nordling, A. Fahlman, R. Nordber, K. Hamrin, J. Hedman, G. Johansson, T. Bergmark, S. E. Karlsson, I. Lindgren, and B. Lindberg, *ESCA—Atomic, Molecular and Solid State Structure Studied by Means of Electron spectroscopy* (Almqvist and Wiksells Boktryckeri AB, Uppsala, 1967; U. S. distributor, Geophysical Corporation of America, Bedford, Mass.), p. 75.

from Pt, Ag and Au and that the position in energy of this structure is in reasonable agreement with structure in the ODS.[2,15,20]

The reason for the lack of structure in the XPS for Cu is not clear at this time; however, it is interesting to note, as will be shown in the next section, that almost the same symmetric curve is obtained in soft-x-ray emission spectroscopy as in the XPS results.

D. Comparison with Results of Soft-X-Ray Emission Spectroscopy

A fourth method used to investigate the valence states of Cu is that of soft-x-ray emission spectroscopy (SXS). The results of such investigations[38,39] are compared in Fig. 21[40] with the ODS. As mentioned in the last section, the SXS curve is very similar to the XPS curve in that it contains a single, almost symmetric peak and shows no evidence of the s- and p-derived states lying between the Fermi level and the top of the d band.

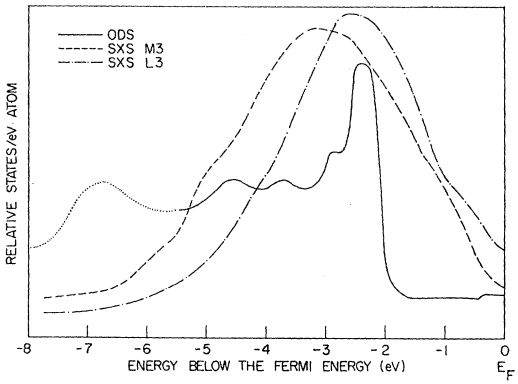

FIG. 21. Comparison between the ODS and results obtained from soft-x-ray emission spectroscopy (SXS) (Refs. 38 and 39). The curve labeled M3 was obtained using M_3 radiation and that labeled L3 using L_3 radiation.

E. Using Rigid-Band Model to Relate ODS of Nickel and Copper

As shown in Fig. 22, our new results for the d-band density of states for Cu and Eastman's new results for the d-band density of states for nickel[7,8] can be relatively well related by a simple rigid-band model, in which the exchange splitting for Ni is taken to be ~0.4 eV. These new findings are in direct conflict with earlier findings,[41]

[38] D. E. Bedo and D. H. Tomboulian, Phys. Rev. **113**, 464 (1959).

[39] Y. Cauchois and C. Bonnelle, in *Proceedings of the International Colloquium on Optical Properties and Electronic Structure of Metals and Alloys, Paris, 1965*, edited by F. Abeles (North-Holland Publishing Co., Amsterdam, 1966), p. 83.

[40] Figure 40 has been taken from Ref. 36.

[41] A. J. Blodgett, Jr., and W. E. Spicer, Phys. Rev. **146**, 390 (1966).

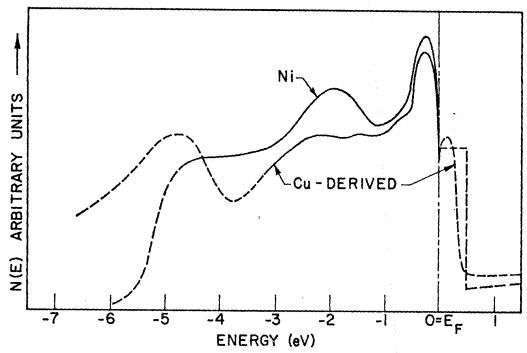

FIG. 22. Comparison of nickel ODS with Cu-derived ODS for Ni, using rigid-band model with an exchange splitting of $\delta E = 0.4$ eV (see Ref. 7).

which were based upon earlier photoemission data in which a lack of sufficient sample purity led to an enhancement of the Ni peak 4.5 eV below the Fermi surface. A more complete discussion of the relationship between the d-band density of states of Cu and the d-band density of states of Ni can be found in Ref. 7.

It should be emphasized that the fact that the nickel and copper ODS can be related via the rigid-band model does not imply that such a model describes the ODS of Ni-Cu alloys. Recent photoemission[42] and theoretical[43] studies show definitively that this is not the case, but rather that the alloys are described by more local models[44,45] such as that of the virtual-bound-state and the minimum-polarity models[43] and not by the rigid-band model.

X. CONCLUSIONS AND DISCUSSION

As stated in the Introduction, a principal object of this work is to subject the model of nondirect-transitions constant matrix elements[46] from the d states of Cu to as stringent a test as possible. The results show that a wide range of experimental data is consistent with this model. In particular, an ODS has been obtained from the experimental studies using the nondirect model. With this ODS the quantum yield, electron-electron scattering length, and numerous energy distributions for clean Cu prepared under ultrahigh-vacuum conditions have been calculated and found to be in good quantitative agreement with experiment. Reasonable agreement is found with other EDC's from films[6] formed under good vacuum conditions for $10.4 \leq h\nu = 20.5$ eV and with EDC's from earlier cesiated surfaces.[2] In addition, reasonably good agreement is obtained between the shape of the calculated and measured ϵ_2's.[47] The position in energy of structure in the ODS correlates well with structure in the calculated density of states of Snow[27] and of Mueller.[28] In view of all of these results, it is clear that the nondirect model accounts well for most of the experimental photoemission and optical data associated with excitation of electrons from the d states of Cu.

In the earlier photoemission study of Berglund and Spicer,[2] a direct transition was observed between the s- and p-derived states near the Fermi surface and a band 4.1 eV above the Fermi surface. The transition occurred near the L point ($L_{2'} \rightarrow L_1$) in the Brillouin zone and is estimated to account for less than 10% of the optical strength. Much of the apparent disagreement between the calculated and experimental ϵ_2 may be due to the fact that no attempt was made to include this direct transition in the calculations. Other direct transitions might occur but might either have final states below the vacuum level (and, hence, not be observable in photoemission) or be too weak to be detected by photoemission against the strong background of nondirect transitions. In his piezoreflectance experiments, Gerhardt[26] has studied in detail two transitions which have the properties expected for direct transitions near the L and X symmetry points of the Brillouin zone. One of these, the direct transition near L, was that mentioned above which had been previously observed and studied in detail[2] by photoemission. The piezoreflectance and photoemission results are in good agreement. No evidence for the direct transition near X ($X_5 \rightarrow X_{4'}$) was obtained in the photoemission experiments of Berglund and Spicer.[2] This might be due to the weakness of this transition. According to Gerhardt,[26] the $X_5 \rightarrow X_{4'}$ transition has small oscillator strength, providing only a tiny hump in his room-temperature measurement of ϵ_2. The fact that the final state of the X transition lies near the vacuum level in cesiated Cu would make a weak transition harder to observe in photoemission than a transition to a higher energy.

Let us now discuss the ODS obtained in this work. For the valence states the ODS gives the probability of an optical transition from those states under the visible and ultraviolet excitation used in these studies. A similar probability has been determined for three other types of transitions based on the techniques of soft-x-ray emission spectroscopy (SXS),[30,38,39] x-ray photoemission spectroscopy (XPS),[36,37] and ion-neutralization spectroscopy (INS).[34] If the transition probability for each method depended only on the valence density of states, each should give that quantity. Since such detailed agreement is not achieved between the four methods, this does not seem to be the case. In Sec. IX the ODS

[42] D. H. Seib and W. E. Spicer, Phys. Rev. Letters **20**, 1441 (1968).
[43] N. D. Lang and H. Ehreinreich, Phys. Rev. **168**, 605 (1968).
[44] L. E. Wallden, D. H. Seib, and W. E. Spicer, J. Appl. Phys. **40**, 1281 (1969).
[45] D. H. Seib and W. E. Spicer (unpublished).
[46] Clearly the matrix elements must decrease as the photon energy becomes arbitrarily large or the sum rule will be violated; however, since so little of the available oscillator strength is used in the photon energy studied here (see Refs. 14 and 24), it is not surprising that the constant-matrix-element assumption works over this restricted photon energy range.
[47] It should be noted that this agreement is obtained despite the fact that the well-established direct transition between s- and p-derived states near L at ~4 eV is not taken into account in the calculation.

is compared to the densities of states obtained from these other methods. The most striking thing about such a comparison is that, whereas the ODS has five pieces of structure (four of which correlate well with structure in the calculated density of states), SXS, INS, and XPS give a single, rather broad peak.

Next, let us make some observations about the relationship between the ODS and the density of states obtained from band calculations. As mentioned earlier, agreement between the calculated density of states and the ODS lies in the correlation in energy of the four principal pieces or groups of d structure (see Figs. 17 and 18); however, there is a considerable difference in peak heights. The position of peaks is certainly the easiest thing in either the photoemission or band calculation to determine correctly; however, one might ask whether one should really expect even this agreement if there are effects beyond the one-electron approximation which remove the importance of $\mathbf{k}$ conservation in the optical transition. Specifically, if the d hole does have any local nature in the excitation event,[48] will this not result in interactions between it and the surrounding electrons (including the excited electron) which would shift the positions in energy of structure? Such interactions are not included in the band calculation,[3] and one might therefore expect a difference between the band calculation and our experimental results. Such a difference might be expected if the band calculation gave the Hartree-Fock ground-state energy states; however, this is not the case. In order for a band calculation to have been found, two minimum requirements have been placed on it.[27,28,49–51] It must give a separation between the top of the d band and the Fermi level, E_{dF}, which is in agreement with the optical excitation energy. It must also give the correct Fermi surface. A critical parameter in determining the Fermi surface is E_{dF}, since it appears as the energy denominator in terms giving the effect of the d interaction at the Fermi surface. Thus, the potentials used in the band calculations take into account, to a certain extent, energy shifts associated with the excitation of an electron from the d band to the Fermi surface. As a result, the good agreement obtained between the experimental and calculated energy levels is not so surprising. The situation for solids can be compared with that for the core levels of atoms, where a difference is found between the Hartree-Fock eigenvalues and the excitation energies.[37]

The disagreement as to relative peak heights is also not so surprising. In the calculations one might expect less agreement between relative peak heights than in peak positions, and there is disagreement in the calculated peak heights of Snow[27] and of Cohen and Mueller.[28] In the ODS, as noted in Sec. III, matrix elements may enhance transitions from initial states at a given energy to all final states.[30,52] This can lead to disagreement between band calculations and the ODS. As was noted in Sec. IX A, the ODS for the s- and p-derived states between the top of the d band and the Fermi level is too high by a factor of 2 or more. This is almost certainly a reflection of a stronger matrix element for these "s- and p-derived" states than that for the d states. At this time, there is no reason to imagine that there will not be a similar variation within the d states themselves. Therefore, it is not surprising that agreement is not obtained between the ODS and band calculations with regard to peak heights.

The source of the structure $\sim$6.7 eV below the Fermi surface in the ODS (see Figs. 4, 17, and 18) is not clear at this time. Before discussing this peak, it is proper that the reader should be warned that the precision with which it can be determined is much less than for the higher-lying structure. It should also be noted that it was not possible to observe it directly in the EDC's from clean Cu prepared in ultrahigh vacuum because of the absorption cutoff of the LiF window used in the vacuum chamber; rather, it was observed from Cu prepared by Vehse and Arakawa[6] in a vacuum of about 10^{-8} Torr (at 10.2 eV the EDC from this sample was not as sharp as that from our samples prepared under better vacuum conditions) and from cesiated Cu.[2] However, since it was clearly present in these two different types of samples, it was included in the ODS.

The band calculations place the bottom of the d states at about -5.5 eV (see Figs. 17 and 18); thus, it does not appear that the structure at ~ -6.7 eV is due to a strong peak in the density of states. Rather, it might be due to the simultaneous excitation of a plasma oscillation and a one-electron excitation as suggested by Nesbet and Grant,[29] to a greatly enhanced matrix element,[30,52] or to other effects.[31]

ACKNOWLEDGMENTS

The authors are grateful for fruitful discussions with C. Fadley, D. Eastman, H. Hagstrum, W. Harrison, F. Herman, F. Mueller, J. C. Phillips, and their colleagues at Stanford University. Thanks are also given to P. McKernan for his work in constructing the photoemission chamber, to B. Schechtman for his assistance in the construction of mechanical equipment, to R. Koyama for his assistance in absolute calibration of the quantum yield, to A. Maurer for his assistance with the computer programming, and to D. Seib for his assistance with this manuscript. In addition, one of us (WFK) would like to express special thanks to Mrs. J. Krolikowski for her constant encouragement and for processing much of the data presented in this paper. The authors are also indebted to D. Eastman, who kindly let us use his unpublished work in our analysis.

[48] Such a resonance or strong scattering nature of the d state could lead to localization of the d hole on a single site for a time comparable to the optical excitation time; in such a case the excited state could not be described in terms of a single Bloch state (see Ref. 3).

[49] B. Segall, Phys. Rev. **125**, 109 (1962).

[50] F. M. Mueller, Phys. Rev. **153**, 659 (1967).

[51] R. A. Ballinger and C. A. W. Marshall, Proc. Phys. Soc. (London) **91**, 203 (1967).

[52] J. C. Phillips (private communication).